Effects of Model Configuration, Flow Conditions and Scale in Modelling Spillway Aeration Grooves

H.-P. Koschitzky, B. Westrich and H. Kobus

Institut für Wasserbau, Universität Stuttgart, Federal Republic of Germany

1 INTRODUCTION

The hydraulic design of spillways with high specific discharge usually requires model investigations. Whereas standard small-scale models are sufficient for the assessment of the general flow pattern, studies on cavitation control by means of aeration have to be conducted in detail models at considerably larger scales /4/, /6/, /7/. Detail models of aeration grooves are studied in order to optimize the geometry and to determine the air entrainment of the grooves. The large model scale necessitates the use of models which represents only a small fraction of the width and length of the spillway. Such sectional models allow only an investigation of a single aeration groove in a given approach flow.

This paper presents a hydraulic model study of the spillway of Laiban Dam on the Philippines, which is part of the Manila Water Supply Project III. Fig. 1 shows the spillway chute, which consists of three sections of different slopes. The upstream weir is ungated and has a width of 60 m, which is reduced by a transitional section to the chute width of 25 m. The horizontal length of the spillway is 397 m with a difference in elevation of 81 m. The spillway chute is terminated by a flip bucket. At the design discharge of 2960 m^3/s the flow velocities in the lower part of the spillway reach values of about 38 m/s. Several aerators are therefore provided (Fig. 1) in order to prevent cavitation damage. Because of greatly differing slopes, two types of aeration grooves are needed (Fig. 2). The objective of the model tests was to ensure the proper hydraulic performance of the aeration grooves and to optimize the geometry such that each aeration groove yields sufficient air as needed for cavitation damage prevention in the subsequent spillway section up to the next aerator. On the one hand, air concentrations near the spillway bottom of 5 to 8% should be reached, which is at present taken to be necessary for cavitation damage prevention /3/, /5/; on the other hand, the air entrainment rates should not become so exceedingly high that the flow depth is markedly increased and hence the side walls become uneconomically high.

2 MODEL DESCRIPTION

The model investigation comprises two hydraulic models with different scales: a sectional model (scale 1:8) and a full width model (scale 1:30).

The sectional model 1:8 contains the air supply system and a section of the spillway corresponding to 2 m in width next to the side wall. It was built of perspex with a length of 6 m (corresponding to 48 m in the prototype) and a width of 0.25 m. The model discharge is supplied by a pressurized conduit with a movable gate at the inlet. The pressure head and the gate opening could be varied independently in order to produce flow Froude numbers with various combinations of water depth and flow velocity. Mean flow velocities from 8 to 13.5 m/s and water depths from 10 to 45 cm were achieved, which results in Froude numbers ranging from 4.0 to 14. In this model different groove geometries were tested and optimized individually.

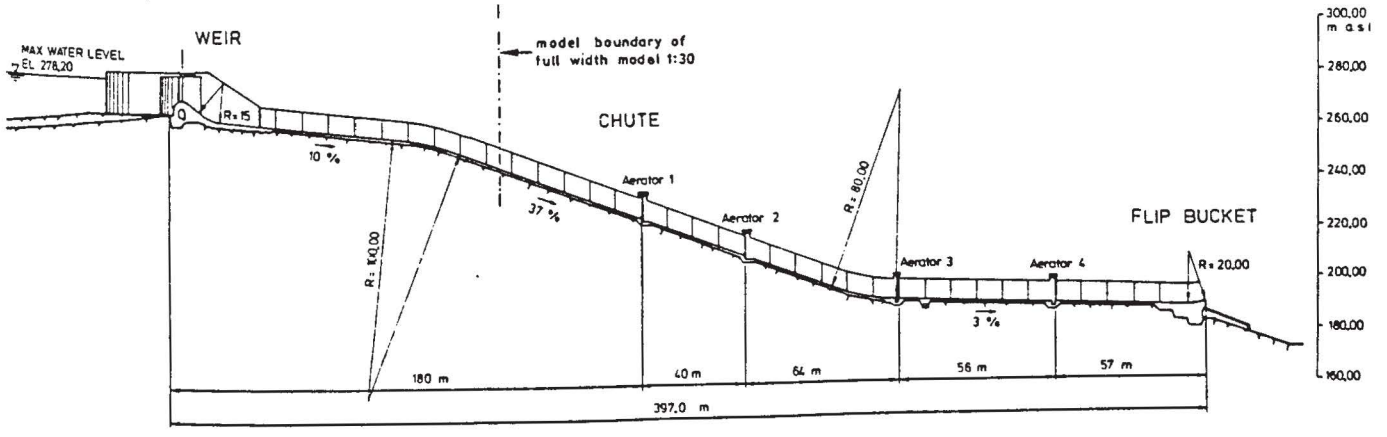

Fig. 1: Laiban Dam Spillway (Philippines)

The full width model 1:30 represents the lower two thirds of the spillway including the four aerators. The flow model boundary is far enough upstream of the first aerator as to provide appropriate approach flow conditions (Fig. 1). The model was also constructed by perspex in order to allow obseryation of the development of the water-air mixture. The following range of hydraulic conditions could be established: mean flow velocities from 4.0 to 6.0 m/s, water depths from 2 to 13 cm, Froude numbers from 4.9 to 10.5. The main goal of the full width model investigations was to clarify the combined function of the aerators with the optimized groove geometry and to observe the flow conditions downstream of the aerators up to the flip bucket.

For both models, water discharges were determined by an in situ calibrated magnetic inductive current meter with an accuracy of less than about ± 0.5%. Air entrainment rates were measured by means of circular nozzles which were mounted on the vertical shaft on either side of each aerator. By a Prandtl tube with a highly sensitive pressure transducer the inflow air velocity in the nozzle was measured and then the air discharge calculated. Several piezometers were installed to measure local pressures in the groove and in the cavity below the jet. The flow depths have been measured by simple point gauges.

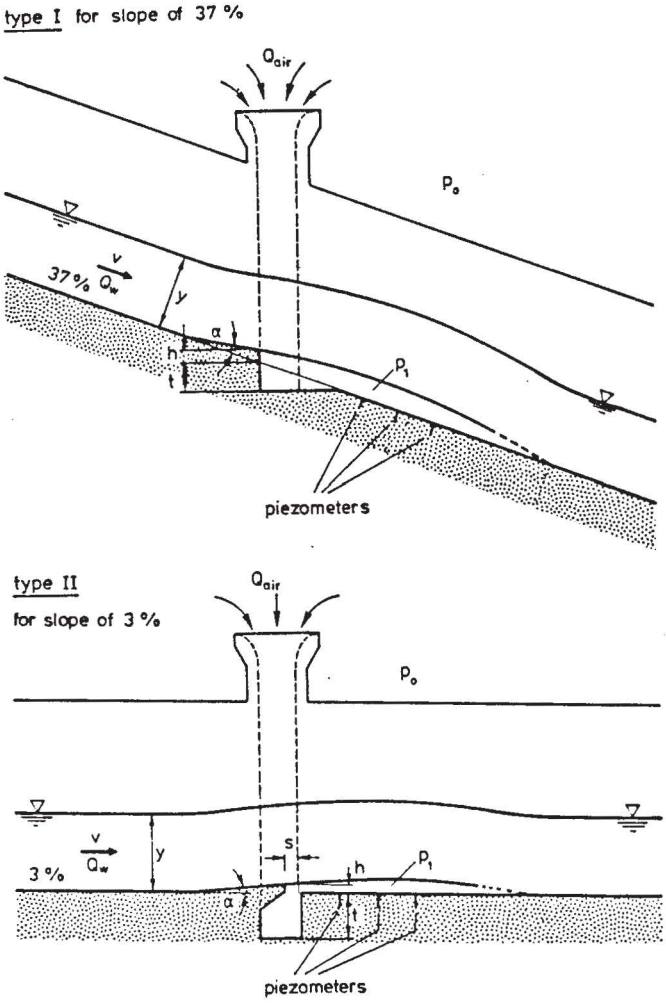

Fig. 2: Definition sketch of the tested aeration grooves

To identify the different parameters which affect the air entrainment mechanism, a dimensional analysis was performed. This yields the following relationship for the air entrainment ratio ß which is to be verified experimentally:

$$\beta = \frac{Q_{air}}{Q_w} = f(Fr = \frac{v}{\sqrt{g \cdot y}};\ c_p = \frac{p_1 - p_o}{\rho v^2/2};\ Re = \frac{v \cdot y}{\nu};$$

$$Z = \frac{\eta^4 \cdot g}{\sigma^3 \rho};\ \text{geometry; approach flow}) \quad (1)$$

For the water model tests, the liquid parameter Z is constant and the same as in the prototype.

The range of the parameter variation in both models are listed in the following table:

	Sectional Model 1:8	Full Width Model 1:30
$Fr \equiv \frac{v}{\sqrt{g \cdot y}}$	4.0 ÷ 14.0	4.9 ÷ 10.5
$c_p \equiv \frac{p_1 - p_0}{\rho v^2/2}$	$-(0.9 \div 3.9) \cdot 10^{-3}$	–
$Re \equiv \frac{v \cdot y}{\nu}$	$(0.9 \div 2.9) \cdot 10^6$	$(0.6 \div 7.0) \cdot 10^5$
$Z \equiv \frac{\sigma^3 \cdot \rho}{\eta^4 \cdot g}$	$40 \cdot 10^9$	$40 \cdot 10^9$

3 MODEL TEST RESULTS FOR A SINGLE AERATION GROOVE

3.1 SPILLWAY SLOPE 37%

In the sectional model tests, given values of the Froude number were verified by various combinations of the velocity v and the water depth y. It was found that the air entrainment ratio $\beta = Q_{air}/Q$ is a unique function of the Froude number, irrespective of the various combinations of v and y. The results are shown in Fig. 3 for a fixed combination of deflector height h and deflector angle α. With an increase of the Froude number, the jumping length increases whereas the impinging angle decreases. Both effects lead to a progressive increase of the air entrainment ratio ß. Obviously, Reynolds number effects are negligible in this case.

Beyond this, the air entrainment increases with increasing magnitude of the deflector angle α and increasing deflector height h (see definitions in Fig. 2). A larger deflector produces a greater jumping length of the jet, which is associated with a more efficient entrainment mechanism.

Corresponding measurements have been carried out in the full width model with the same deflector height (h = 20 cm) and deflector angle (α = 5.2°). Measurements were taken for aerator 1 and also for aerator 2 after complete removal of the upstream aerator 1. Thus the approach flow conditions in terms of local Froude number, Reynolds number and turbulence intensities for both aerators were comparable. The full width model test results confirm the unique dependence of the ß-value upon the Froude number (Fig. 3). The sectional model data are plotted without any width correction, which is justifiable for

this groove type because of the negligibly small pressure losses in the air supply system. It can be seen from Fig. 3 that the air entrainment rates of the two models show a systematic but small difference of nearly the same order of magnitude as the measurement accuracy. If the different pressure losses in the air supply systems were taken into account, the results of both model tests would move even closer together. Therefore, it may be concluded for this case that scale effects and the effects of using a sectional model are not significant.

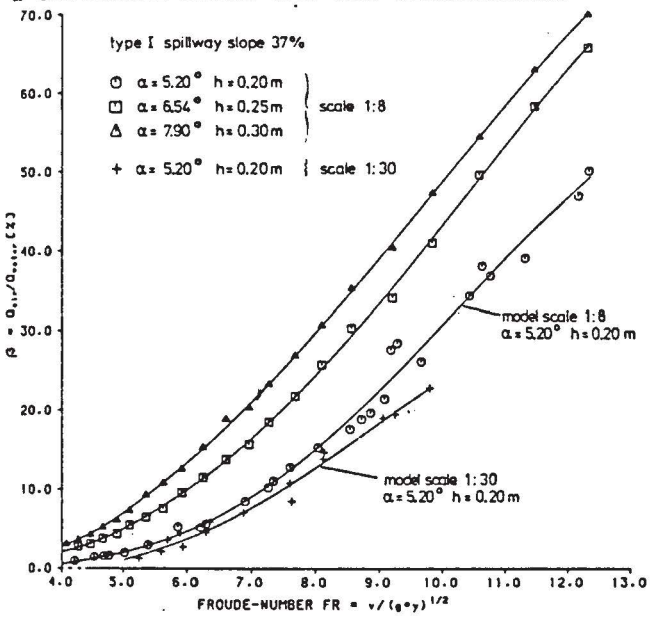

Fig. 3: Relationship between air entrainment ratio ß and Froude number Fr for aeration groove type I. Results of scale models 1:8 and 1:30

3.2 SPILLWAY SLOPE 3%

For the 3% slope spillway section a different type of aeration groove had to be designed. Because of the different geometry, a larger pressure head loss in the air supply system and therefore considerable negative pressures below the jet are to be expected. The jet trajectories are affected strongly by the pressure difference ($\Delta p = p_1 - p_0$) between the atmosphere and the air cavity below the jet. Since the air entrainment mechanism reacts sensitively to the pressure gradient at the impinging point, the pressure losses in the air supply system have to be considered as a significant boundary condition. In dimensionless form, this is expressed by the pressure parameter c_p as defined in Eq. (1).

In Fig. 4, experimental results from the sectional model 1:8 are shown in terms of a diagram of the air entrainment ratio ß as a function of the Froude number Fr with the pressure parameter c_p as third parameter. All these data pertain to a fixed aeration groove geometry. In the lower Froude number range (Fr < 7), the air discharge through the air supply system is relatively small and hence also the resulting pressure differences are small. Therefore, an influence on the air entrainment is not measurable in this range, and hence the experimental data tend to coincide on a single curve. In the upper range of Froude numbers, however, there is a significant influence of the pressure parameter as indicated by the solid lines which correspond to different values of c_p. With increasing pressure difference, the jet length decreases and the impinging angle increases. Furthermore, the air has to overcome a higher pressure gradient at the impinging point, so that all in all it is plausible that at a given Froude number the air entrainment ratio ß will decrease with increasing values of the pressure parameter c_p.

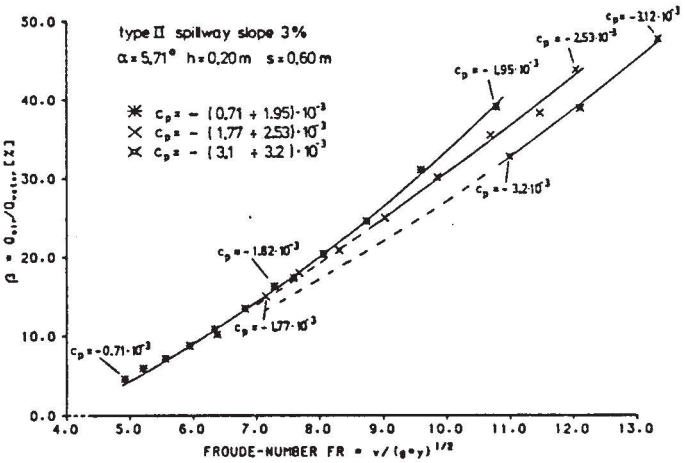

Fig. 4: Relationship between ß and Froude number for aeration groove type II indicating the influence of the relative pressure difference c_p

From the application point of view, it is desirable to compensate these undesired pressure effects by a proper hydraulic design of the groove geometry, which produces a lower pressure head loss and thereby an increase of the air entrainment for the same flow conditions. As the pressure loss in the air flow system is mainly due to the sharp 90° corner of the horizontal groove, breaking this corner and increasing the slot widths from 60 to 80 cm has substantially decreased the pressure head losses. The experimental investigation has shown that the pressure losses of the final geometry were so small that no noticeable influence of c_p was found in the entire range of Froude numbers investigated. Thus, the change in groove geometry has led from the relationship given in Fig. 4 to the results shown in Fig. 6.

It is to be noted that in the sectional model the air flow is not modelled correctly /4/, /7/. As the water discharge in the sectional model is only 8% of the total discharge, the air discharge through the air supply system will be correspondingly small compared to the total air discharge. In the full width situation, the higher air flow rate will cause higher pressure head losses for the given air supply geometry. In order to account for this effect, the air pressure has to be adjusted artificially to account for the reduction of the spillway width. In lack of desirable prototype information, the pressure adjustment procedure has been based upon the following assumption. The pressure head loss of the air flow within the aeration groove, i.e. from the side wall to the spillway axis, is considered negligibly small compared to the local losses in the air supply shafts and hence to the total pressure head loss in the air supply system; consequently the air entrainment rate per unit width is assumed to be constant. Then it follows that the total air discharge for a single air shaft (feeding half the spillway width) has to be 6.25 times larger than measured in the sectional model. The pressure head losses in the air supply system are proportional to the square of the air discharge for turbulent flow.

Therefore, the pressure head loss has to be increased by a factor $\sqrt{6.25} = 2.5$ in order to compensate for the actual air discharge in the full width spillway. This so-called "full-width correction" was realized in the sectional model by a throttle in the air supply system.

The aeration groove type II has been tested in the sectional model to determine the air discharge Q_{air} depending on the undisturbed approach flow conditions, i.e. the Froude number, and the air supply conditions, i.e. pressure head $\Delta p/\gamma$. For a given aerator geometry, Fig. 5 shows the results for different throttlings of the air inflow. The throttling is determined by the pressure loss coefficient ξ of the air supply system which is defined as follows:

$$\xi = \frac{p_o - p_i}{\rho v_{air}^2/2} \qquad (2)$$

The characteristics of the air supply system correspond to a given value of ξ (solid lines). The dashed lines indicate the relation between $\Delta p/\gamma$ and air discharge for constant water flow conditions (v, y = const.) which were obtained by changing the throttling of the air supply: they represent the air entrainment characteristics of the water flow .

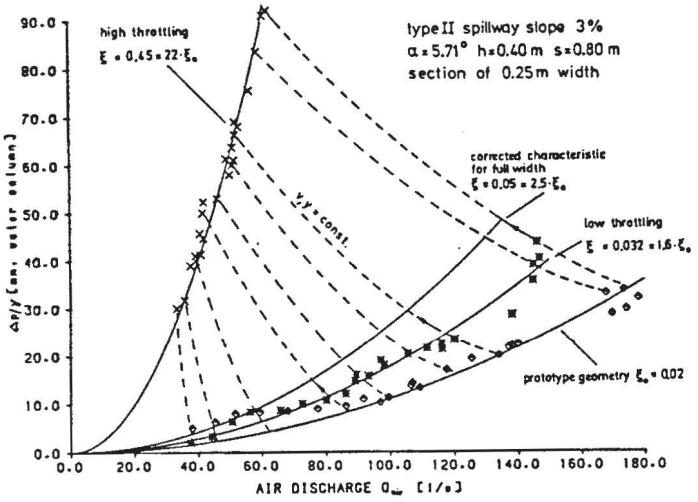

Fig. 5: Characteristic of air supply system for aeration groove type II measured in the sectional model scale 1:8

The experimental data clearly show that for a given water flow (v, y = const.) the air discharge Q_{air} increases with decreasing throttling of the air supply (decreasing ξ) and correspondingly decreasing pressure head difference $\Delta p/\gamma$. In the extreme case of no pressure loss, the air discharge would be controlled exclusively by the characteristics of the supercritical water flow: these conditions would yield the maximum possible air discharge.

For the prototype geometry, the original experimental data from the sectional model 1:8 are represented by the line for (ξ_o = 0.02) in Fig. 5. In order to transfer these data to the prototype, the "full-width correction" has to be applied, which leads to the line of ($\xi = 0.05 = 2.5\ \xi_o$). Now the actual air entrainment can be determined as the intersection point of the characteristics of the air supply system and the air entrainment characteristics of the flow. It can be seen from Fig. 5 by following the dotted line of constant flow characteristics that the full width correction results always in a higher pressure difference and a smaller air discharge as compared to the uncorrected sectional model data. This underlines the fact that a simple geometrical width correction without proper consideration of pressure changes can lead to considerable errors.

After having established correct water flow and air flow conditions in the sectional model 1:8, the experimental data can be compared with those of the full width model 1:30. Such a comparison is shown in Fig. 6 for the aeration groove type II tested at the location of aerator 3 with an undisturbed approach flow (complete removal of the upstream aerators 1 and 2). The diagram shows the experimental results of the sectional model 1:8 without any correction (upper line) and with full width correction (middle line) as well as the corresponding data from the full width model 1:30 (lower line). Beyond the confidence intervall of the measuring points, there is a systematic difference between the two models which clearly exceeds the range of measurement accuracy has to be attributed to scale effects. The air entrainment ratio ß is higher in the larger model, i.e. the air entrainment mechanism is more efficient in the large scale model. The reason for this may be some difference of the pressure parameter c_p in both the models. Because the pressure loss in the model 1:30 is very difficult to measure, unfortunately this cannot be confirmed by measuring data.

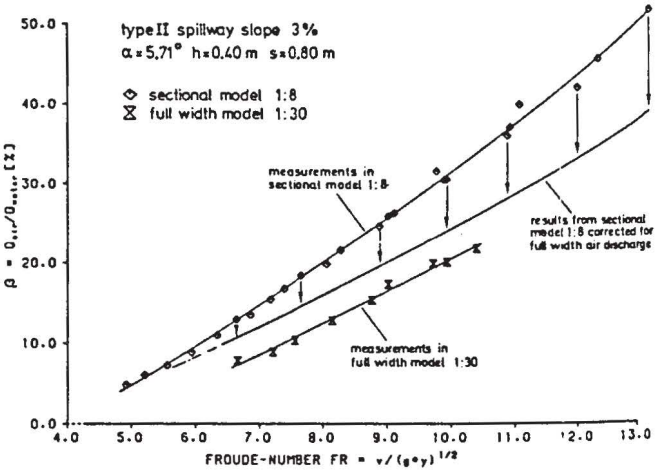

Fig. 6: Comparison of the relationship between ß and Froude number for the sectional model 1:8 and the full width model 1:30

4 AIR ENTRAINMENT OF CONSECUTIVE AERATION GROOVES

All experimental data described so far refer to a single aeration groove in undisturbed approach flow conditions. These conditions are only realized for the upstream aerator 1. The three subsequent aeration grooves experience different approach flow conditions which affect their air entrainment rate, so that the single aeration groove results cannot be applied directly. For the subsequent aerators, additional hydraulic factors have to be considered, which can be summarized as follows:

- Each aerator acts as a local disturbance and turbulence generator, which causes a local energy loss leading to a reduction of the flow Froude number downstream;

- each aerator has its individual air entrainment rate, which changes the subsequent flow characteristics;

- the local disturbance by aerators seems to be high enough in order to initiate free surface self-aeration immediately in the vicinity of the first aerator. This self-aeration mechanism is important because it provides a smaller decay of the air concentration at the spillway bottom which is important for cavitation damage prevention.

All these factors are interacting and it is not yet well understood how these affect quantitatively the performance of subsequent aerators. As a first step, several experiments were performed on the full width model 1:30 in order to show the influence of the approach flow conditions on the air entrainment rate of the aerator 2 (type I) and aerator 3 (type II). The results are shown in Fig. 7.

For aerator 2, results are given for the air supply of aerator 1 being open or closed, in comparison to measurements in undisturbed approach flow, for which the aerator 1 was completely removed. It is seen that at higher flow rates the presence of the aerator 1 enhances air entrainment, and that closing off the air supply at aerator 1 increases the entrainment at aerator 2. This trend is reversed, however, in the range of low flow rates.

The measurements at aerator 3 also show that closing off the air supply of the upstream aerators leads to an increase of the entrainment at high flow rates and to a decrease at low flow rates.

These reversals in trends indicate that several counteracting effects are present. It seems that at least at low flow rates the air entrainment is enhanced by the presence of air bubbles in the approach flow, whereas at the high flow rates the local energy losses and the associated increase in turbulence production may become dominant.

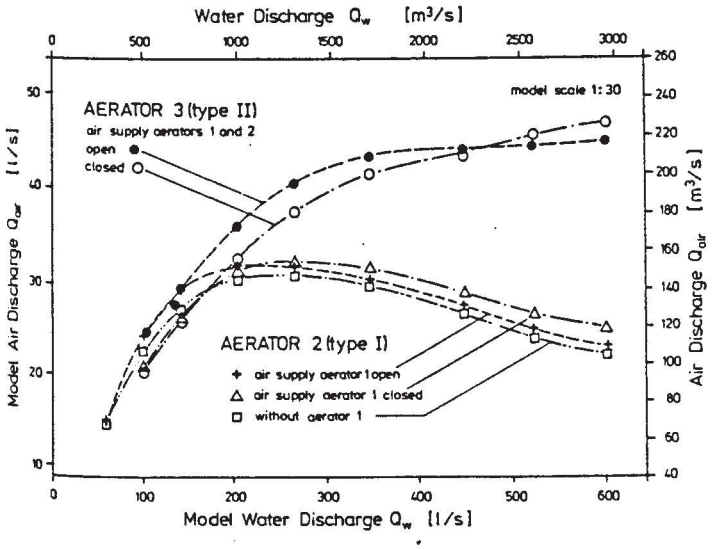

Fig. 7: Influence of upstream flow conditions on the air demand of aerators 2 and 3

5 CONCLUSIONS

From the laboratory investigations of a spillway chute in two models of different scale (1:8 and 1:30), some conclusions about scaling and modelling effects can be drawn:

- The air entrainment ratio ß is a unique function of the flow Froude number $Fr = v/\sqrt{g \cdot y}$, regardless of the absolute value of velocity v and water depth y.

- The unique relation ß and Fr holds as long as the pressure loss in the air supply system is negligibly small and does not influence the air entrainment rate. However, in case of an air supply system with energy losses the magnitude of ß decreases with increasing values of the pressure parameter c_p.

- In sectional models, a full width correction for the air inflow rate is necessary. This can be provided by a corresponding adjustment of the pressure losses in the air supply system leading to the correct value of c_p.

- For undisturbed approach flow conditions, i.e. for the first aerator, the air entrainment is not affected by the scale of the Froude model provided the flow Reynolds number is larger than about 10^5. Open questions remain, however, about scale effects when air pressure losses are significant.

- For the subsequent aerators, the air entrainment is influenced by the complex interaction between turbulence and air bubbles in the approach flow.

REFERENCES

/1/ Cain, P.; Wood, I.R.: Measurements of Self-Aerated Flow on a Spillway. ASCE HY11, November 1981

/2/ Kaveshnikov, A.T.; Lentyaev, L.D.: Flow Aeration on the Operating Spillway at the Sayano-Shushenskioe Hydroelectrical Station. Hydrotechnical Construction. pp. 12-19. January 1978

/3/ Peterka, A.J.: The Effect of Entrained Air on Cavitation Pitting. Proceedings Minesota International Hydraulics Convention, USA. September 1953

/4/ Pinto, N.L. de S.; Neidert, S.H.: Model Prototype Conformity in Aerated Spillway Flow. International Conference on the Hydraulic Modelling of Civil Engineering Structures. Coventry, England. September 22-24. 1982

/5/ Quintela, A.C.: Flow Aeration to Prevent Cavitation Erosion. Water Power & Dam Construction, January 1980

/6/ Vischer, D.; Volkart, P.; Siegenthaler, A.: Hydraulic Modelling of Air Slots in Open Chute Spillway. Int. Conference on the Hydraulic Modelling of Civil Engineering Structures. Conventry, England. September 1982

/7/ Volkart, P.; Chervet, A.: Air Slots for Flow Aeration - Determination of Shape, Size and Spacing of Air Slots for the San Roque Dam Spillway. Proceeding of the Laboratory of Hydraulics, Hydrology and Glaciology, No. 66, Zürich. 1983